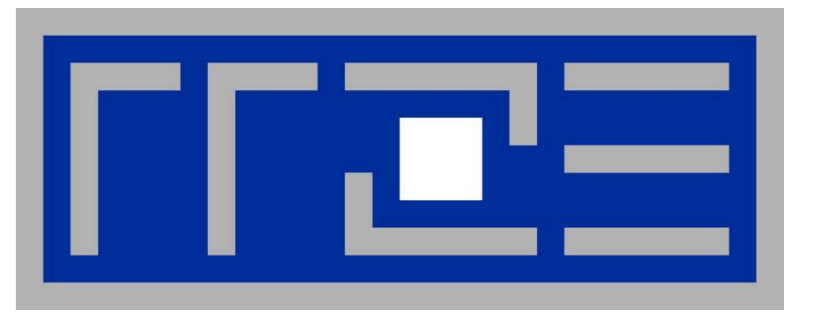




Disorder effects in graphene: A local distribution approach

Jens Schleede¹, Gerald Schubert^{1,2} and Holger Fehske¹

¹ Ernst-Moritz-Arndt Universität Greifswald, ² Regionales Rechenzentrum Erlangen



Motivation

Among the most remarkable features of graphene are the linear dispersion in the vicinity of the band centre and its true two dimensional (2D) structure. Preparing technologically relevant samples (nanoribbons), two additional aspects influence the material properties: disorder and boundary effects. The presence of disorder in 2D systems leads to Anderson localisation (AL) of the electronic wave function. In finite, weakly disordered devices the localisation length may become comparable or even larger than the system size, leading to conducting behaviour despite the localisation of the wave function. The competition between boundary effects, localisation length and system size triggers the technologically relevant questions:

- How much disorder can we tolerate in a sample without destroying the conducting behaviour?
- How do the ribbon edges influence this value?

Models

Disordered graphene nanoribbons

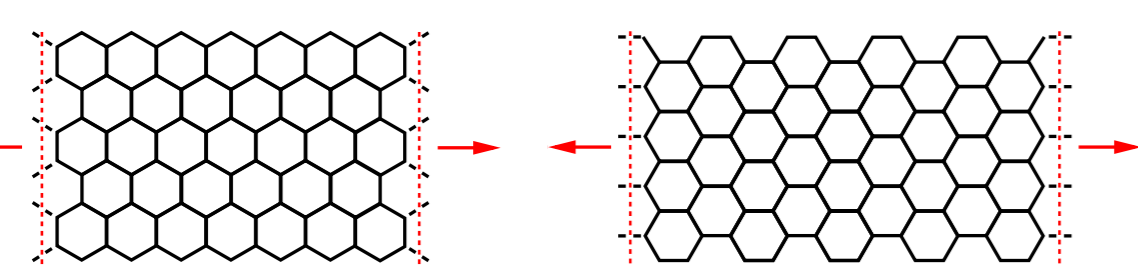
Investigating the localisation properties of the single particle wave function in graphene, we consider the tight-binding Hamiltonian

$$H = \sum_{i=1}^N \epsilon_i c_i^\dagger c_i - \bar{t} \sum_{\langle ij \rangle} (c_i^\dagger c_j + \text{H.c.})$$

on a honeycomb lattice with N sites, including hopping between nearest neighbours $\langle ij \rangle$ only. Choosing the on-site potentials ϵ_i from the box distribution

$$p[\epsilon_i] = \frac{1}{\gamma} \theta \left(\frac{\gamma}{2} - |\epsilon_i| \right),$$

we introduce Anderson-type disorder into the model. We consider quasi-1D systems with finite widths and open boundaries in the transversal direction, whereas the other boundary conditions are periodic. Depending on the orientation of those ribbons with respect to the honeycomb lattice, we have to distinguish the cases of zigzag and armchair geometries:



Zigzag (left) and armchair (right) graphene nanoribbons.

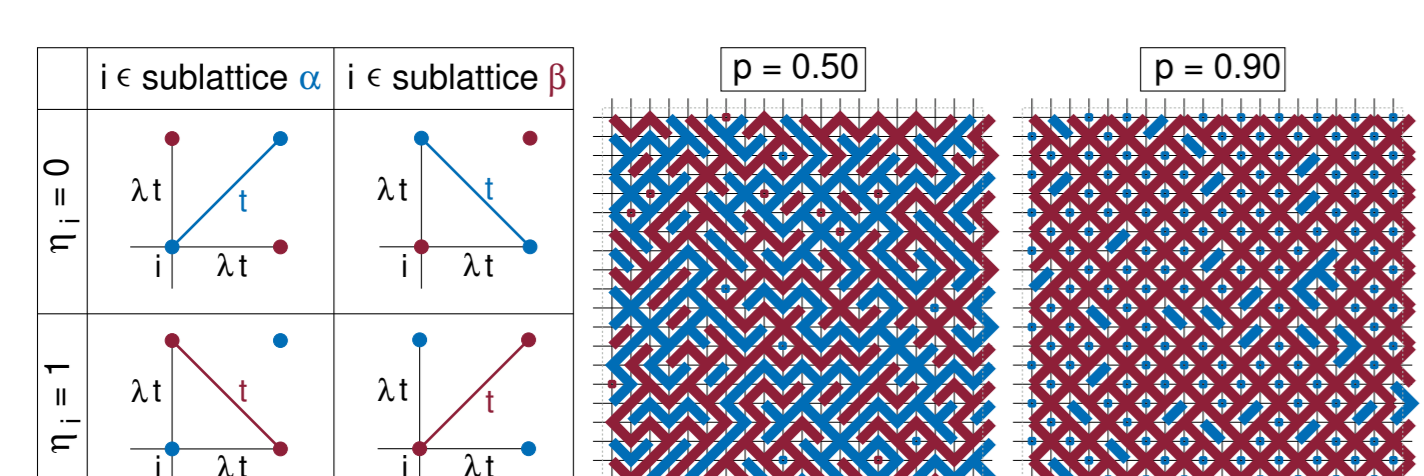
Furthermore, we single out the difference between bulk and edge disorder, whereby we account for different ribbon widths and edge geometries.

Quantum RRN model

Mesoscopic regions of different charge carrier density may arise in graphene sheets because of, e.g., inhomogeneities in the substrate or non-perfect stacking [1]. In order to model the minimal conductivity in graphene, a random resistor network (RRN) representation of a graphene sheet has been proposed by Cheianov *et al.* [2]. Thereby random links between electron and hole “puddles” (corresponding to lattice sites) are assumed to determine the observed conductivity rather than the local conductivity of a puddle. Extending the 2D quantum site-percolation model by including a finite “leakage” κ between all lattice sites, the Hamiltonian reads

$$H = -\bar{t} \left[\sum_{i \in \alpha} (\eta_i c_{i+\gamma}^\dagger c_i + (1 - \eta_i) c_{i+\gamma}^\dagger c_{i+\gamma}) + \sum_{i \in \beta} (\eta_i c_{i+\gamma}^\dagger c_i + (1 - \eta_i) c_i^\dagger c_{i+\gamma}) + \kappa \sum_i (c_i^\dagger c_{i+\gamma} + c_i^\dagger c_{i+\gamma}) \right] + \text{H.c.}$$

The two sublattices α and β represent, e.g., regions of different charge carrier concentrations. Those regions are randomly connected; the $\eta_i \in \{0, 1\}$ determine the present diagonal in each plaquette. Between suchlike linked sites, the hopping probability is much higher than for nearest neighbours (reduced by $\kappa < 1$). Tuning the expectation value of the $\{\eta_i\}$ -distribution, $p = \langle \eta_i \rangle$, controls the size of connected regions.



Left: Generation rule for the RRN model. Sublattices α and β form a bipartite checkerboard on the 2D square lattice. Right: Particular realisations of the RRN for $p = 0.5$ and $p = 0.9$.

Methods for detecting AL

The large localisation lengths in disordered 2D systems necessitate the investigation of system sizes beyond reach of exact diagonalisation (ED) methods. Instead, we apply Chebyshev expansion based techniques, requiring only matrix vector multiplications of a state with the (sparse) Hamiltonian. The local distribution approach for the local density of states (LDOS) allows for an energy resolved investigation of the localisation properties of the single particle eigenstates. In addition, we propagate an initially localised wave packet by applying the time evolution operator in order to substantiate our findings.

Local distribution approach

(Alvermann, Fehske, J. Phys. Conf. Series, **35**, 145 (2006))

In a given sample of a disordered system translational invariance is broken. The local properties of site i are reflected in the LDOS,

$$\rho_i(E) = \sum_{m=1}^N | \langle i | m \rangle |^2 \delta(E - E_m).$$

Recording the probability density function $f[\rho_i]$ for many different sites $\{i\}$ of a certain sample and different sample realisations $\{\epsilon_i\}$ restores translational invariance on the level of distributions: The shape of $f[\rho_i]$ is determined by $p[\epsilon_i]$ (i.e. by γ) but independent of $\{i\}$ and $\{\epsilon_i\}$. For extended states, $f[\rho_i]$ is a normal distribution and independent of the system size, whereas for localised states we have a log-normal distribution which tends to become singular for increasing system sizes [3]. Normalising the LDOS to its mean value, $\rho_{me} = \langle \rho_i \rangle$, allows for a detection of the localisation properties by performing a finite size scaling for the LDOS distribution or the cumulated distribution function, $F[\rho_i] = \int_0^{\rho_i} f[\rho'_i] d\rho'_i$. More conveniently, the typical DOS $\rho_{ty} = e^{\langle \ln \rho_i \rangle}$ monitors the changes in the shape of the LDOS distribution. While for $N \rightarrow \infty$ an extended state is characterised by finite values of ρ_{me} and ρ_{ty} , for localised states ρ_{me} is finite but $\rho_{ty} \rightarrow 0$.

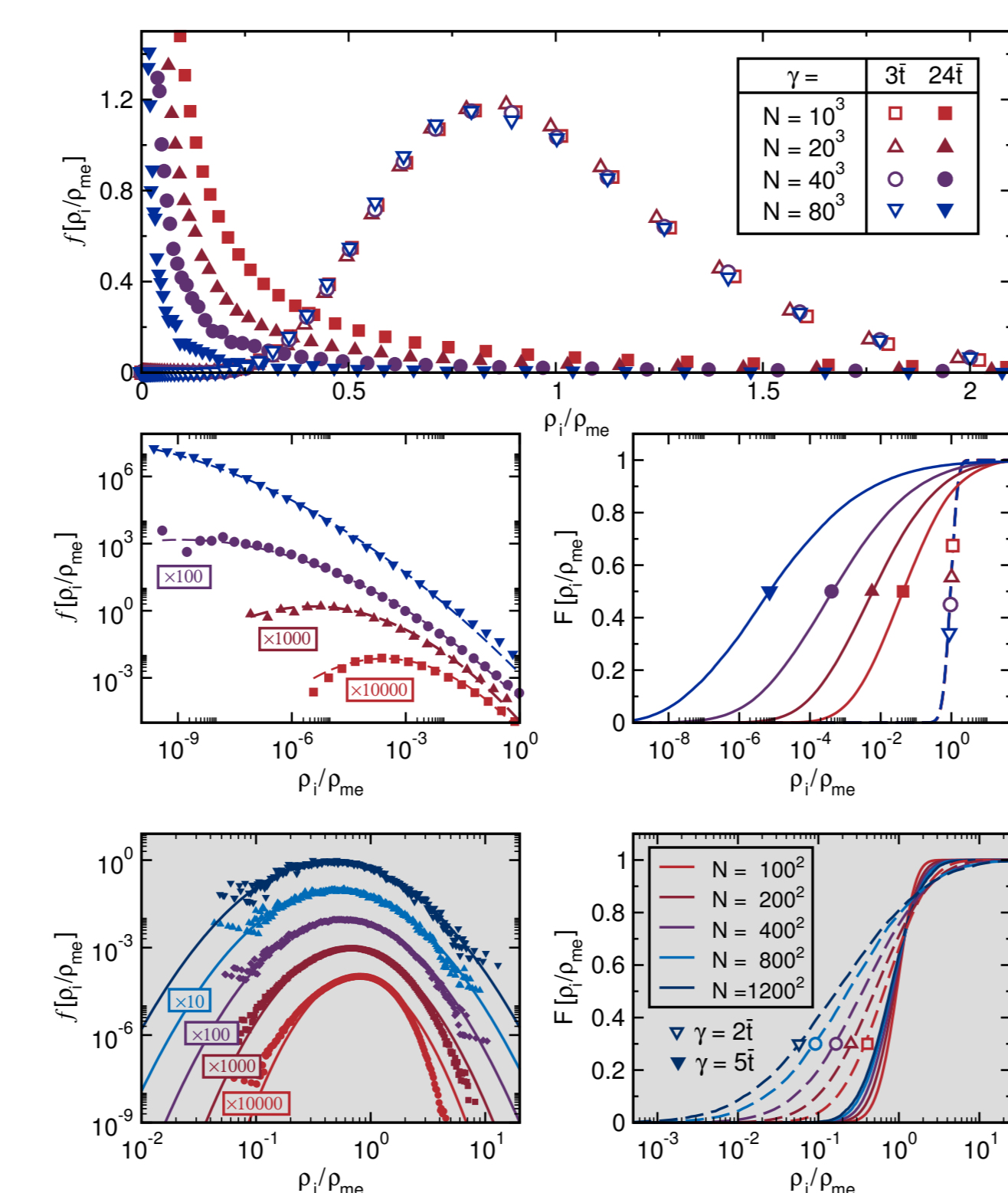


Illustration of the local distribution approach on the basis of the Anderson model on a 3D (upper two rows) and 2D (bottom row) lattice. For 3D, we compare the dependency on the system size for weak ($\gamma = 3t$) and strong ($\gamma = 24t$) disorder. Extended states: more or less uniform amplitudes of the wave function $\sim f[\rho_i]$ sharply peaked and symmetric around ρ_{me} . Localised states: ρ_i strongly fluctuates throughout the lattice $\sim f[\rho_i]$ is very asymmetric with a long tail and $\langle \rho_i \rangle \rightarrow 0$. The data is extremely well described by a log-normal fit. For 2D we also find localised behaviour but at much larger length scales.

Chebyshev expansion

(Weiße, Wellein, Alvermann, Fehske, RMP **78**, 275 (2006))

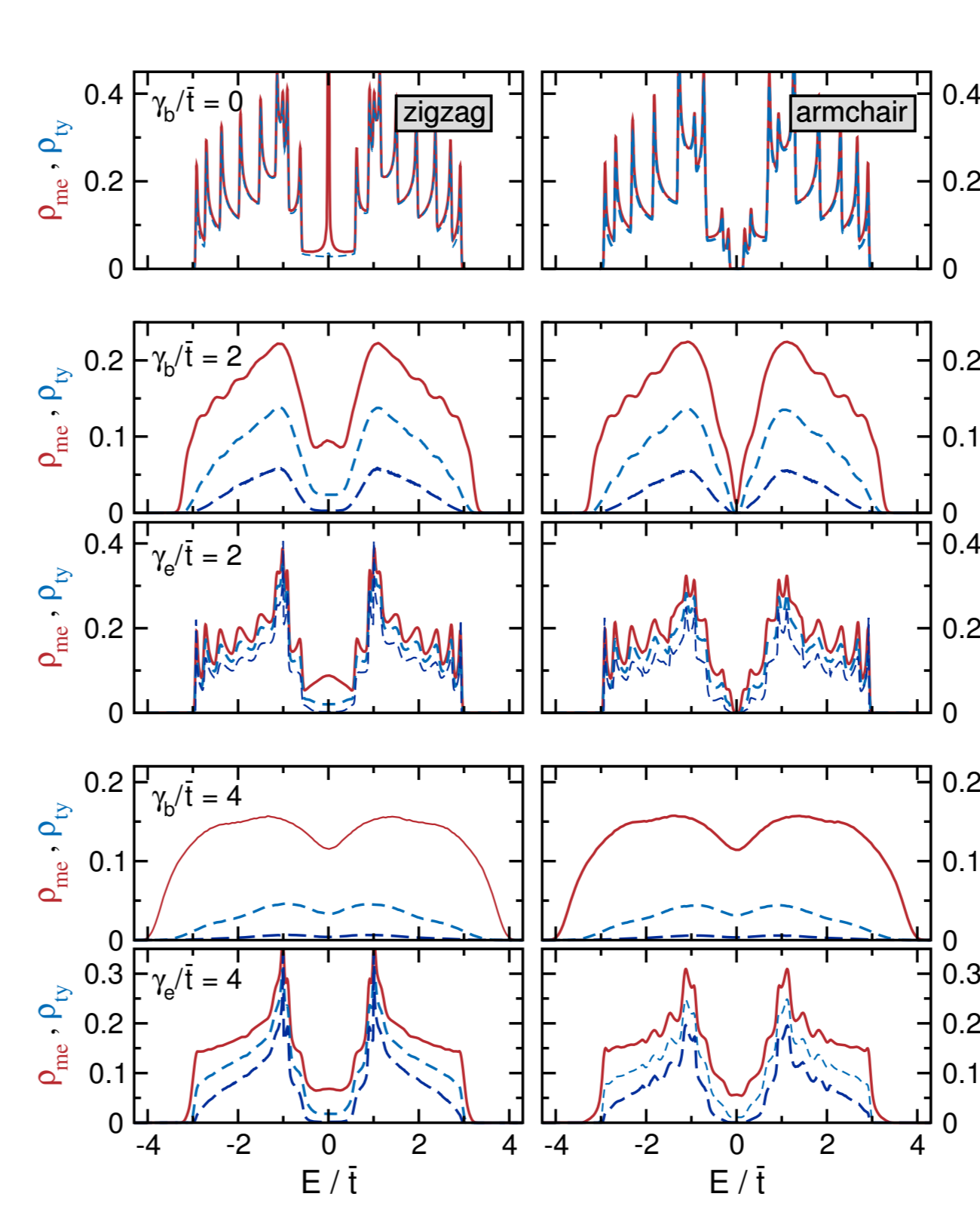
Alternatively, the recurrence probability $P_R(t)$ in the limit $t \rightarrow \infty$ also reveals the localisation properties of the system. While in the thermodynamic limit $P_R \sim 1/N \rightarrow 0$ for extended states, localised states are characterised by a finite value of P_R . Starting from a localised wave packet, we calculate the time dependent local particle density,

$$n_i(t) = |\psi(\mathbf{r}_i, t)|^2 = \left| \sum_{m=1}^N e^{-iE_m t} \langle m | \psi(0) \rangle \langle i | m \rangle \right|^2,$$

by expanding the time evolution operator into a finite series of Chebyshev polynomials. Also for $n_i(t)$ the local distribution approach applies. But since any initial state in general contains contributions of the whole spectrum, examining $n_i(t)$ does not allow for an energy resolved investigation of localisation as the LDOS. Instead it provides a tool for a global examination of the spectrum with relevance for possible measurements. A finite overlap of already one extended state with the initial state leads to a complete spreading of this state after some time.

Results

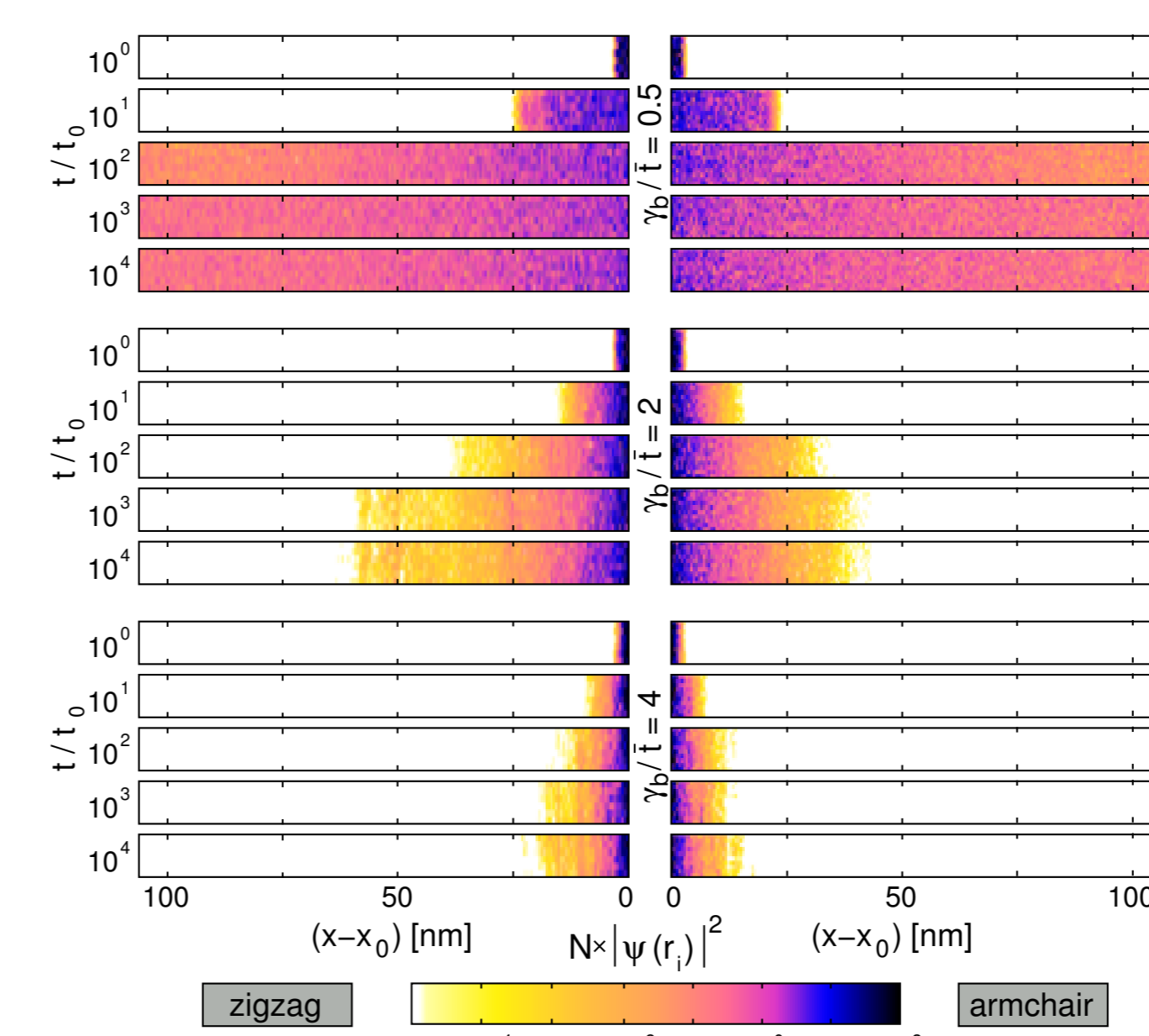
Edge versus bulk disorder in GNRs



Mean and typical DOS for zigzag (left column) and armchair (right column) ribbons of width $W = 1.1$ nm. We compare the influence of edge to bulk disorder for two disorder strength. To illustrate the localisation properties, in each panel ρ_{ty} is given for $L = 213$ nm and $L = 2128$ nm.

• In contrast to zigzag and $N_a = 3n$ armchair ribbons, the DOS for other (ordered) armchair ribbons is gapped at $E = 0$. Introducing disorder, localised states emerge in the gap. Above a critical disorder strength γ^c the gap vanishes, with $\gamma_e^c > \gamma_b^c$.

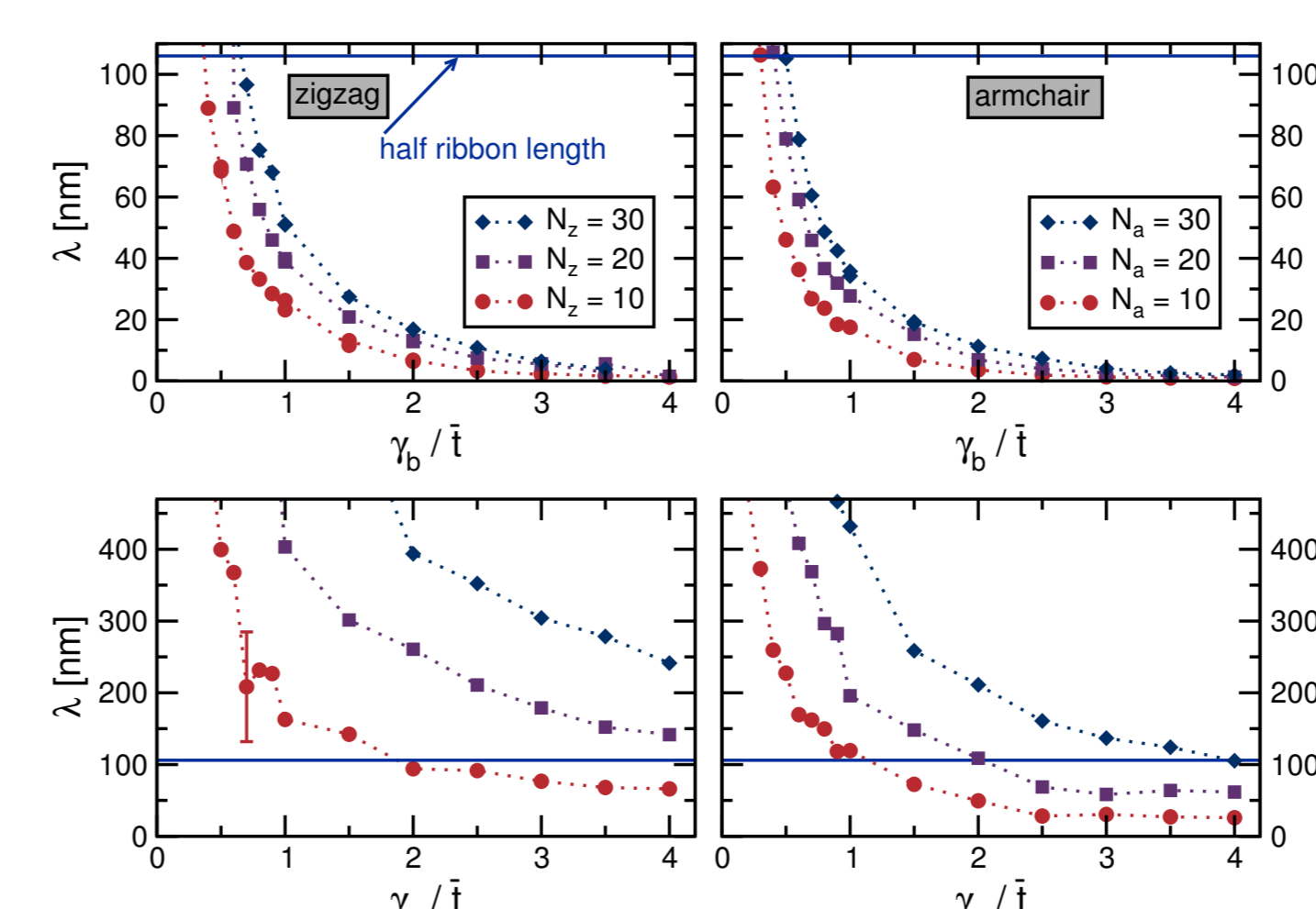
• Analysing ρ_{ty} reveals the localisation properties: The reduced values of ρ_{ty} indicate localisation throughout the band for both ribbon geometries and the shown values of bulk disorder. Weak edge disorder cannot localise the wave function on short armchair ribbons as indicated by the approximate agreement of ρ_{ty} and ρ_{me} . Only for larger systems ρ_{ty} is substantially reduced, pointing towards localisation.



Time evolution of an initially localised wave packet on disordered zigzag and armchair ribbons for different values of bulk disorder γ_b . Shown is the normalised particle density $N|\psi(\mathbf{r}_i, t)|^2$. Device dimensions: $(1.1 \times 213) \text{ nm}^2$ with $N \approx 10^4$ atoms.

• After a fast spreading process, the maximum extension of the wave function does not change anymore, even for very long times. On individual sites the amplitudes fluctuate with time, giving the shown state a “quasistationary” nature.

• The localisation length depends both on disorder strength and edge geometry. Armchair ribbons are more susceptible to the presence of disorder than those of zigzag type (shorter λ for the same γ_b). Ribbons of moderate length and weak disorder: $\lambda > L \sim$ wave function spreads over the whole ribbon.

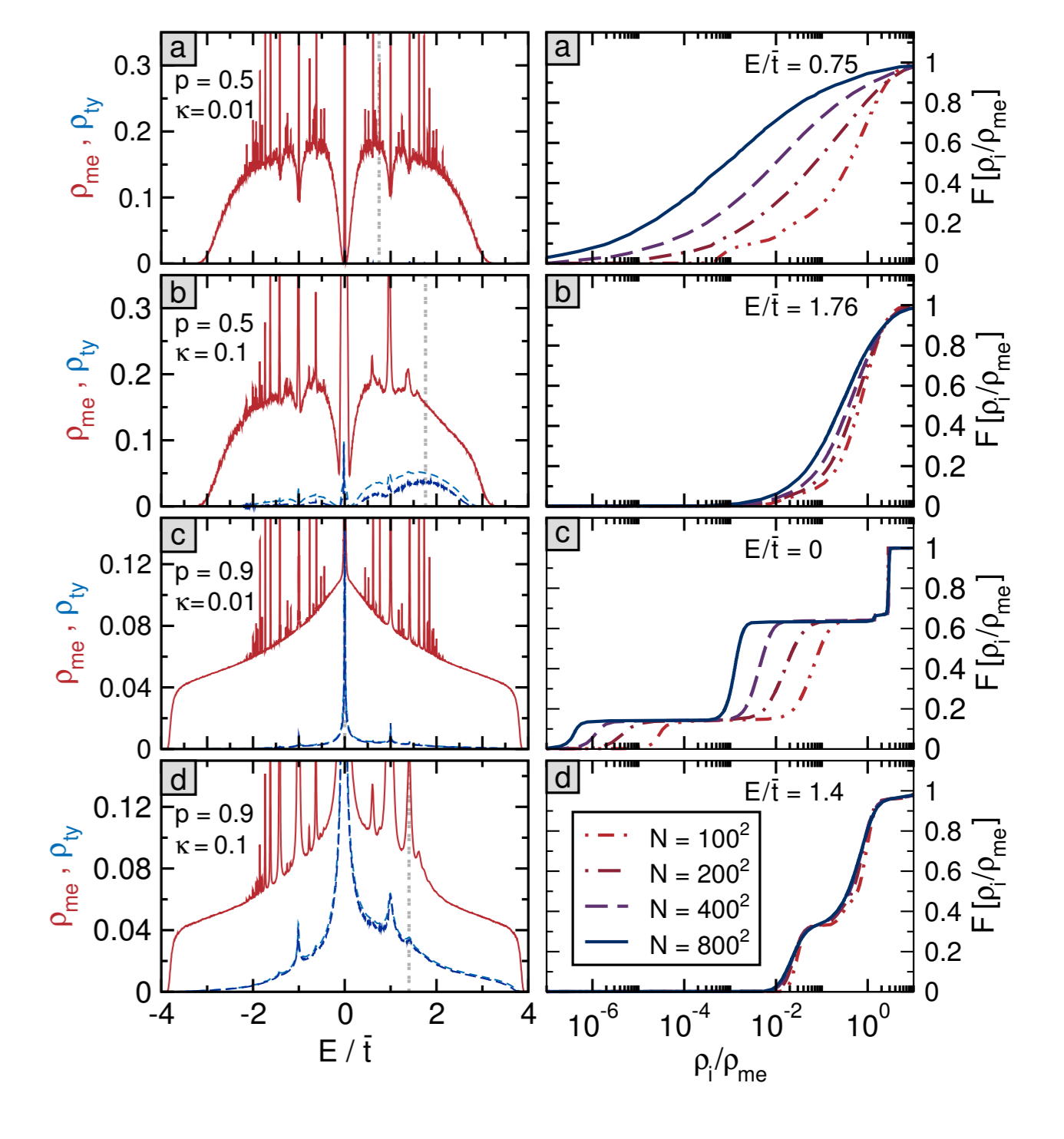


Localisation length λ on zigzag and armchair ribbons ($L = 213$ nm) as a function of bulk and edge disorder strength.

• Even though Anderson localisation takes place in 2D disordered systems for any $\gamma > 0$, the finite extension of the systems calls for a more in-depth consideration. For a given ribbon size we can estimate up to which disorder a given sample is metallic.

Leakage effects in RRNs

(Schubert & Fehske, PRB **78**, 155115 (2008))

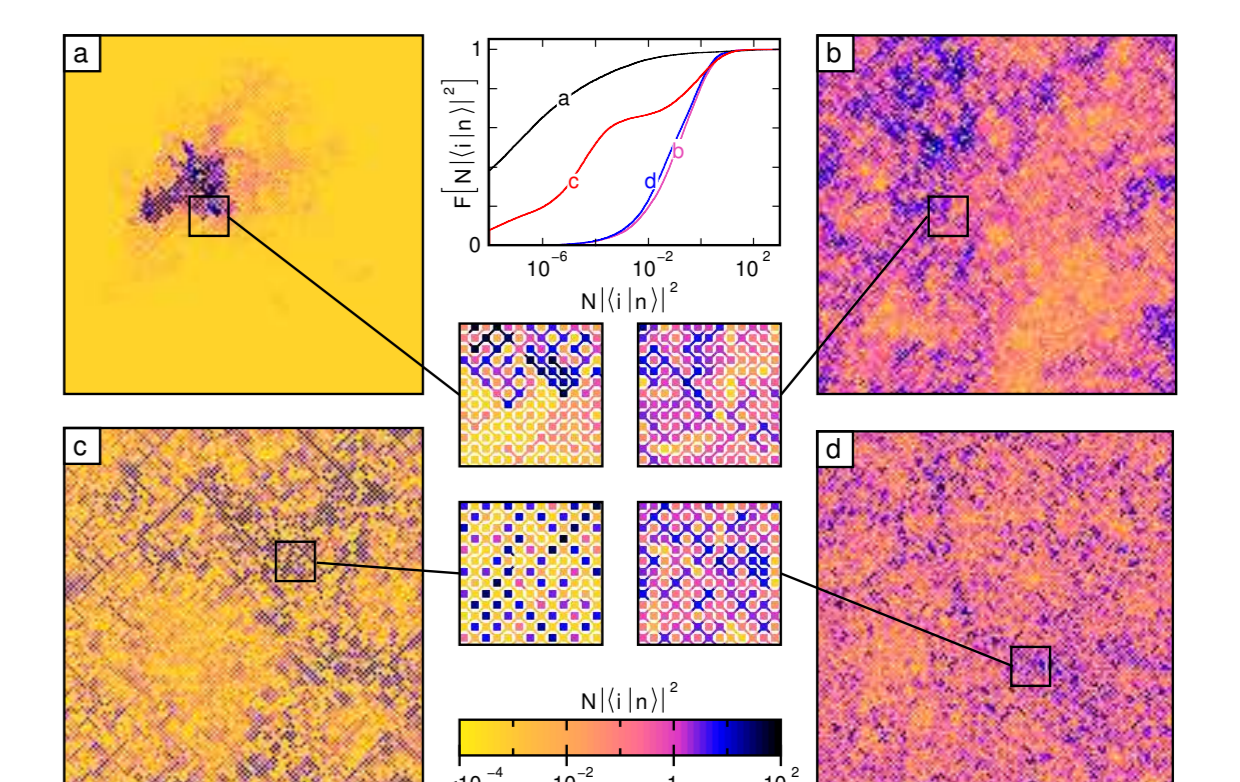


Left: Mean and typical DOS for the RRN model on a $N = 400^2$ lattice. For comparison ρ_{ty} is also given for $N = 800^2$. Right: Size dependence of $F[\rho_i/\rho_{me}]$ at certain energies (indicated by the vertical dashed lines in the left panels).

• The inclusion of next-nearest neighbour hopping causes a pronounced asymmetry that grows with increasing κ . The multitude of spikes can be attributed to localised states on “isolated” islands, getting less probable for increasing κ . As compared to the quantum percolation model, the presence of κ shifts those special energies.

• For small κ all states are localised (vanishing ρ_{ty}), except for the band centre in (c). There, the two-step structure of $f[\rho_i/\rho_{me}]$ gives a hint to a bimodal (checkerboard) structure of the wave function.

• The finite, system size independent ρ_{ty} for larger κ points towards extended states. The reduction as compared to ρ_{me} can be explained by the sublattice structure and leakage effects.



Normalised occupation probability $N|\langle i | n \rangle|^2$ of characteristic eigenstates $|n\rangle$ on a $N = 128^2$ RRN-lattice as obtained by ED. Same parameters (p, κ, E_n) as in the previous figure.

• Panel (a) shows a localised state. For large κ , the amplitudes in (d) fluctuate over the whole lattice without any global structure, indicating an extended state. In contrast, the additional structures on intermediate scales in (b) suggest localisation on large length scales.

• For case (c) we observe the checkerboard structure of the amplitudes. The two-step structure in $F[N|\langle i | n \rangle|^2]$ is less pronounced than for $F[\rho_i/\rho_{me}]$. While ρ_i takes into account the whole eigenspace, here only one eigenstate of the $E = 0$ subspace is shown.

Conclusions

By means of the local distribution approach we were able to distinguish localised from extended states for two disordered tight-binding models, in particular for transport models for graphene. Anderson localisation is identified by a log-normal distribution of the LDOS that shifts towards zero for increasing system size. The localisation length for weakly disordered graphene nanoribbons may be larger than the system size, leading to conducting behaviour. Also in a RRN model, aiming at modelling the influence of charge inhomogeneities, we found conducting states, for which the existence is mainly triggered by the leakage rate between the regions of different charge carrier concentrations.

[1] E. Rossi, S. Das Sarma, Phys. Rev. Lett **101**, 166803 (2008);
M. I. Katnelson, A. K. Geim, Philos. Trans. Roy. Soc. Lond, Ser. A **366**, 199 (2008);
J. H. Chen, C. Jang, M. S. Fuhrer, E. D. Williams, M. Ishigami, Nature Phys. **4**, 377 (2008)
[2] V. V. Cheianov, V. I. Fal'ko, B. L. Altshuler, I. L. Aleiner, Phys. Rev. Lett. **99**, 176801 (2007)
[3] G. Schubert, A. Weiße, G. Wellein, H. Fehske in „High Performance Computing in Science and Engineering“ edited by S. Wagner, W. Hanke, A. Bode, and F. Durst, pp. 237 (2005)